Advanced Composite Materials

ISSN: 0924-3046 (Print) 1568-5519 (Online) Journal homepage: http://www.tandfonline.com/loi/tacm20

Acoustic emission monitoring of multiaxial ultimate elastic wall stress tests of glass fibre-reinforced epoxy composite pipes

M.S. Abdul Majid, M. Afendi, R. Daud, A.G. Gibson, T.A. Assaleh, J.M. Hale & M. Hekman

Advanced Composite Materials, 2015
Vol. 24, No. 1, 1–16, http://dx.doi.org/10.1080/09243046.2013.871175

Acoustic emission monitoring of multiaxial ultimate elastic wall stress tests of glass fibre-reinforced epoxy composite pipes

M.S. Abdul Majid[a]*, M. Afendi[a], R. Daud[a], A.G. Gibson[b], T.A. Assaleh[b], J.M. Hale[b] and M. Hekman[c]

[a]*School of Mechatronic Engineering, Universiti Malaysia Perlis (UniMAP), Bangunan KWSP, Jalan Bukit Lagi, 01000 Kangar, Perlis, Malaysia;* [b]*Mechanical and Systems Engineering, Newcastle University, Stephenson Building, Newcastle upon Tyne NE1 7RU, UK;* [c]*Technology & Engineering Developments Future Pipe Industries (FPI), P.O. Box 1371, Dubai, United Arab Emirates*

(*Received 28 August 2012; accepted 23 July 2013*)

This paper describes the acoustic emission (AE) monitoring of multiaxial ultimate elastic wall stress (UEWS) tests of filament wound glass fibre-reinforced epoxy composite pipes under hydrostatic, pure axial and pure hoop loadings at room temperature. The purpose of AE monitoring is to quantitatively identify and characterise damage inception and evolution, which leading to different failure mechanisms via an analysis of AE parameters. AE parameters such as counts and energy released were plotted against time, and changes of these AE activities were monitored. A 3D correlation plot between AE amplitude and duration against time for each loading condition was produced and analysed. The AE measurement of both hydrostatic and pure axial loading suggested that matrix cracks were initiated early in the tests and possible had progressed into delamination failure just before UEWS point was reached at 200 MPa of hoop stress and 63 MPa of axial stress, respectively. No clear damage initiation and progression was observed for pure hoop loading condition. Significant AE events were only noted when buckling induced delamination and debonding failure, which followed by fibre fracture at the outer surface of the pipe.

Keywords: polymer-matrix composites (PMCs); strength; acoustic emission; filament winding; matrix cracking; ultimate elastic wall stress (UEWS)

1. Introduction

During the biaxial loading of glass fibre reinforced epoxy (GRE) pipes, Hull [1] reported that minutes before weepage was observed, the formation of white streaks was always accompanied by a creaking noise. This creaking sound is an acoustic emission (AE) indicating the cracking process involved.

Composite materials, as do many other materials, emit acoustic signals under load if elastic stresses are reduced by plastic deformation or the initiation of cracks. These emissions correspond to the strain energy due to microstructural changes. Once these emissions reach a threshold level, they can be detected and converted into a voltage signal by a piezoelectric transducer. The signals can then be amplified and measured to produce data such as frequency, energy release and duration of the signals. Each signal emitted is recorded in real time and associated with a specific event over time. The AE

*Corresponding author. Email: shukry@unimap.edu.my

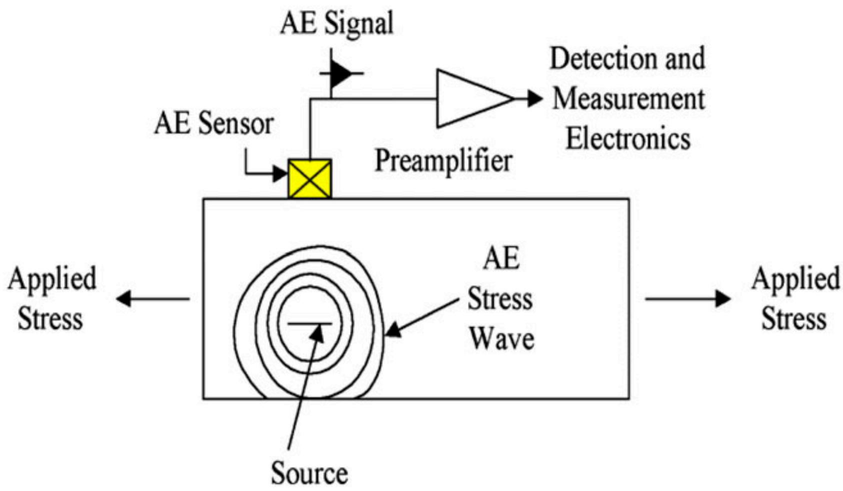

Figure 1. Basic principal of AE.[24]

and detection process is illustrated in Figure 1. A typical AE signal or event is shown in Figure 2. Each event can be described by several parameters such as amplitude, counts, energy counts, duration and rise time.

The study of failure mechanisms of composite materials by means of AE has increasingly been becoming of interest in recent times due to its potential to be employed in safety application in marine, automotive and especially in aerospace industries. William and Lee and Guild et al. [2,3] were one of the earliest researchers to have

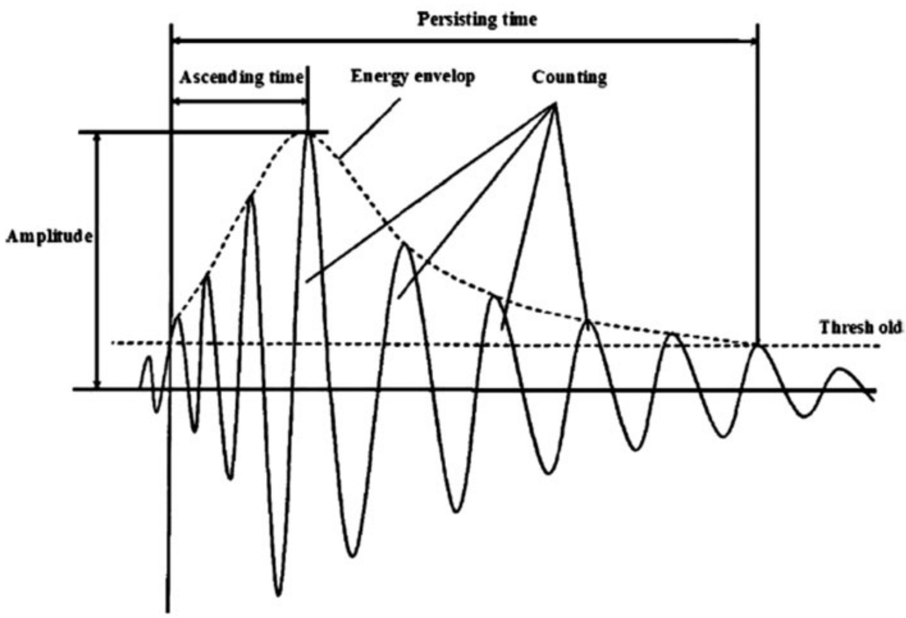

Figure 2. Common parameters from acoustic signals.[13]

suggested AE as mean for monitoring the damage mechanisms in composite materials. Giordano et al. [4] conducted the quantitative failure analysis on polymer-reinforced composites via analysis of AE parameters to investigate the types of damage in composite laminates. More recently, Yu et al. [5] conducted damage detection in composite laminates through characterisation of the real-time acoustic frequency. Others include work by Huguet et al. [6] and Godin et al. [7] who studied extensively the use of AE procedure to determine the inception and progression failure modes in glass/polyester composites.

Of late, there has been increasing interest in the prospect of using AE monitoring to detect the fatigue performance of GRE pipes. This is due to the presence of multiple failure mechanisms of matrix cracking, delamination and fibre breakage all of which generate specific distinguishable frequencies. Hence, the technique is not only of potential use in determining the point of failure, but also in determining its nature. Barre and Benzeggagh [8] tested glass fibre-reinforced polyester and concluded that AE amplitudes vary with different failure modes. They found that AE amplitudes in the range of 40–55 dB correspond to the matrix cracking, 60–65 dB to debonding, 65–85 dB to fibre pull-out and 85–100 dB to fibre fracture.

Barnes and Ramirez [9] conducted a study of static and fatigue loading on carbon fibre-reinforced pipes and used correlation plots of event duration and amplitude to characterise the damage mechanisms. They reported that low-amplitude events are normally characteristic of matrix cracking, high duration, low/intermediate amplitude events with debonding and delamination, while high amplitude with short duration is typically attributed to fibre breakage. Czigany [10] through his investigation has demonstrated that it is possible to correlate AE parameters such as number of events, amplitude and energy to the mechanical properties during various applied loadings. A very comprehensive literature review was conducted by Rosa et al. [11] on the application of AE technique for damage mechanisms detection and progression for natural fibre composites.

Khalifa and co-workers [12] performed mechanical characterisation of glass/vinylester composite pipes under axial loading by AE technique and tension test. The AE responses were found to distinctly correspond to the four damage modes observed in tension test: matrix cracking, interface debonding, delamination and fibre breakage. Most recently, Liu et al. [13] used AE technique to investigate the damage mechanisms and progression of carbon fibre-reinforced epoxy laminates. They found that the amplitude for matrix cracking, fibre/matrix interface debonding, delamination and fibre pull-out and breakage is about 40–60, 50–70, 60–80 and 80–110 dB, respectively.

Prevorovsky et al. [14] recorded acoustic signals from multiaxial tests on GRE pipes combining internal pressure and axial tensile loading. Highest AE activity was recorded during tension cycles while pressure testing. They went on to identify matrix microcracking and delamination as the main damage mechanisms in the test. Later work by Ramirez et al. [15] investigated the endurance limits to weepage for GRE pipe under internal pressure using AE techniques and static pressure tests. Their results suggest that AE monitoring can be used to predict the long-term cyclic loading performance of GRE products from a single short-term test. If this were proven, it would potentially reduce the amount of fatigue testing required to qualify products. In addition, AE can also be used for a rapid evaluation of the factors that affect fatigue performance, such as changes in raw materials, fabrication processes or fitting design. Nevertheless, the implementation of such technique requires a clear understanding of relationships between the AE parameters recorded and the associated damage mechanisms.

In this work, the damage mechanisms took place during the ultimate elastic wall stress (UEWS) tests were characterised via AE technique. In order to produce a full service condition at room temperature (RT), acoustic data were recorded from three UEWS tests: pure axial loading (0:1), giving a negative transverse to shear stress ratio; hydrostatic pressure (2:1) which results in a high transverse to shear stress ratio; and finally, pure hoop loading (1:0) which yields a high shear to transverse stress ratio.

2. Experimental

GRE pipes for the UEWS tests conducted in the experiments were provided by Future Pipe Industries (FPI) from their standard range of Wavistrong wound pipes. The pipes were manufactured from glass fibre impregnated with aromatic amine (MDA) cured epoxy resin.[16] Table 1 shows the physical and mechanical properties of the tubes. The pipes were manufactured by a conventional automated winding machine with a winding angle of ±55° for optimum working conditions under internal pressurisation. The wall of the pipes is protected on the outer side by the resin topcoat. Figure 3(a) shows the dimensions of the specimen agreed with (FPI) for this investigation for hydrostatic, pure axial and pure hoop tests at RT. The parallel length of the pipe used in the test, not including the fitting region, was about 1600 mm. The pipes were designed with built-up, tapered end reinforcement.

The UEWS test involves the application of groups of 10 one-minute hydrostatic pressure cycles at increasing pressure levels. The strain at the end of the first and the last cycle of each 10 cycle group is measured, and these values are plotted against pressure (or hoop stress). If zero or negligible damage occurs at a particular pressure level, then a linear relationship is observed between strain and hoop stress, and the strain after the 10th cycle in the group is the same as at the first cycle. As the UEWS is approached, a deviation in strain can be seen between the first and the last cycle, and the relationship begins to become nonlinear. This nonlinearity in the stress–strain relationship will then be used to indicate the UEWS point, which corresponds to first ply failure in the pipe. Further details on the UEWS test procedure and the calculations involved are given in recent paper by Abdul Majid et al. [17]

Table 1. Mechanical and physical properties of the GRE pipes provided for this investigation by FPI.[16]

Internal diameter	200 mm
Average wall thickness	6 mm
Length	2000 mm
Liner	n/a
Density	2000 kg/m^3
Number of plies	10
Glass volume fraction	59%
Axial tensile modulus	11.5 GPa
Hoop tensile modulus	19.0 GPa
Shear modulus	11.0 GPa
Major Poisson's ratio,	0.65
Coefficient of linear thermal expansion	2×10^{-5} mm/mm °C
Thermal conductivity	0.29 W/m.K
Specific heat	921 J/kg.K

In hydrostatic (2:1), pure axial (0:1) and pure hoop (1:0) loadings of UEWS tests at RT, the AEs were monitored and recorded using an AE instrument manufactured by the Physical Acoustics Corporation with 150 kHz resonant sensors. Two sensors were placed on the outer surface of the pipe with a layer of silicone grease and secured using Sellotape. The signals picked up by the sensors were strengthened to higher voltage using a preamplifier, which was placed close to the sensors in order to minimize electromagnetic interference. The AE set-up is shown in Figure 3(b). After the sensor was fixed and connected to the acoustic software, simple 'lead break' calibration was carried out to ensure that the signal received was consistent and the sensor properly secured to the pipe surface. The process involved breaking a lead pencil near the sensor to verify the response from the acoustic sensors. If the latter were properly attached, the lead breaks should give a reproducible signal throughout. To eliminate background noise and unrelated signals from the data, the acoustic signal threshold was set at 40 dB, which meant that only events with hits above 40 dB were recorded. The AE data were continuously recorded throughout the UEWS test, and line marks were made to

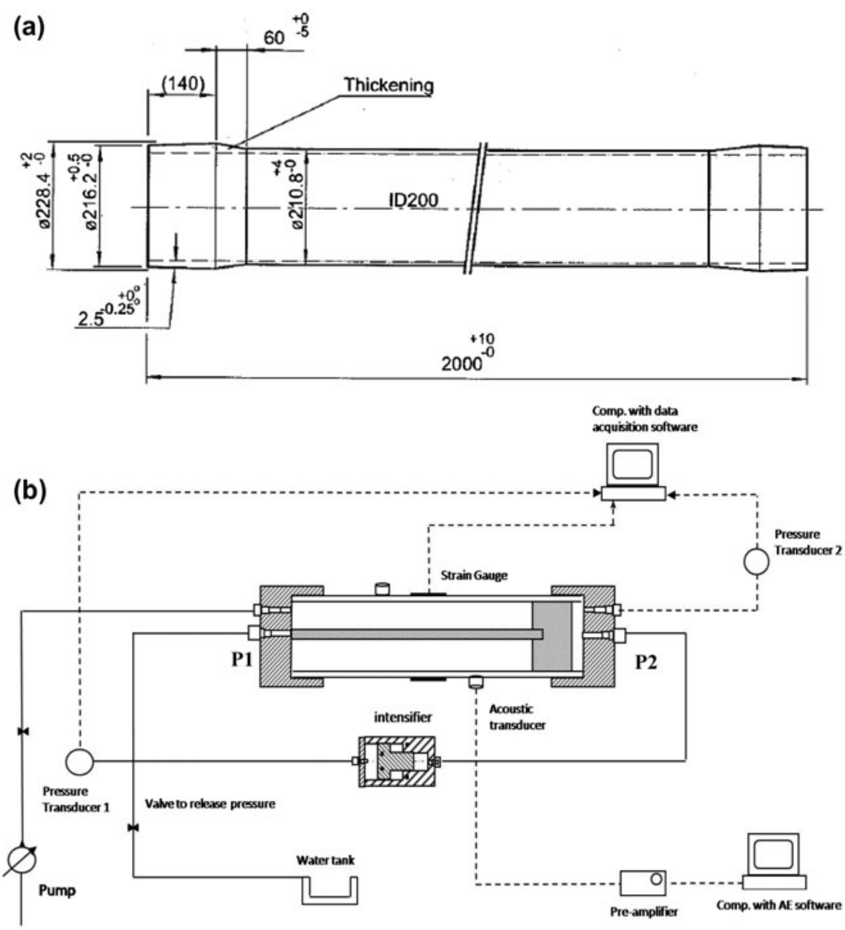

Figure 3. (a) dimensions (in mm) of the GRE pipe used in the UEWS tests and (b) schematic drawing of test rig for conducting UEWS test showing the set-up of acoustic sensors.

differentiate the cycle groups of increasing pressure. AE monitoring was continued until weepage failure was observed.

3. Results and discussion

UEWS tests under three conditions were chosen for this AE investigation; pure hydrostatic loading at 2:1 hoop to axial stress ratio and pure axial and pure hoop loadings at 0:1 and 1:0 stress ratio, respectively, to achieve full service condition. These test conditions also represent failure mechanisms that were governs either by transverse tensile stress (0:1) or shear stress (1:0) or combination of both (2:1). Table 2 gives the UEWS results of the aforementioned conditions. Details such as changes in the appearances of the surface of the pipe, fracture orientation or matrix failure were meticulously recorded. Types of failure modes observed could be categorised into three different modes: tensile axial failure in pure axial loading, weepage failure in pure hydrostatic loading and localised leakage failure in pure hoop loading. Details of these failure modes observed and its mechanisms were discussed in detail from previous paper published by the author in [17].

3.1. Pure hydrostatic loading (2:1)

Figure 4 shows the recorded AE response with respect to the number of counts and cumulative energy against time during the UEWS test at the 2:1 loading ratio. The wall stress (MPa) applied in each cycle group is indicated at the top of the plots. Figure 5 shows the weepage failure and the micrograph image of the pipe wall after weepage failure showing the transverse matrix cracking. As illustrated in Figure 4(a), the AE counts started very early in the low pressure cycle groups. Activity then slowly increased as the pipe was loaded in the next cycle group with increased pressure. Notable increases in AE counts were observed in the 4th cycle group with pressure at 48 bars, which corresponds to 74 MPa indicating the first significant change in AE activity. This is believed to be the result of the initiation of matrix cracking. In the next three cycle groups, AE counts more or less stabilised, which suggests a constant rate of damage progression. Another significant increase in AE counts was noted in the 7th cycle group with a wall stress of 130 MPa where the event counting reaches about 12,000 at roughly 11,000 s. This sudden increase in AE count is likely to correspond to substantial transverse matrix cracking and the progression of interface debonding, which then possibly led to a change in damage mechanism from matrix cracking to delamination.

Figure 4(b) shows the cumulative energy plot against time with the corresponding wall stress indicated at the top of the plot. The AE activities recorded suggest that damage initiation and progression were taking place in close proximity to transducer 2.

Table 2. UEWS test results for 2:1, 0:1 and 1:0 loading ratios.[17]

UEWS experimental results		
	Room temperature	
Stress ratio (hoop:axial)	Hoop stress (MPa)	Axial stress (MPa)
0:1	0	63
2:1	200	100
1:0	265	0

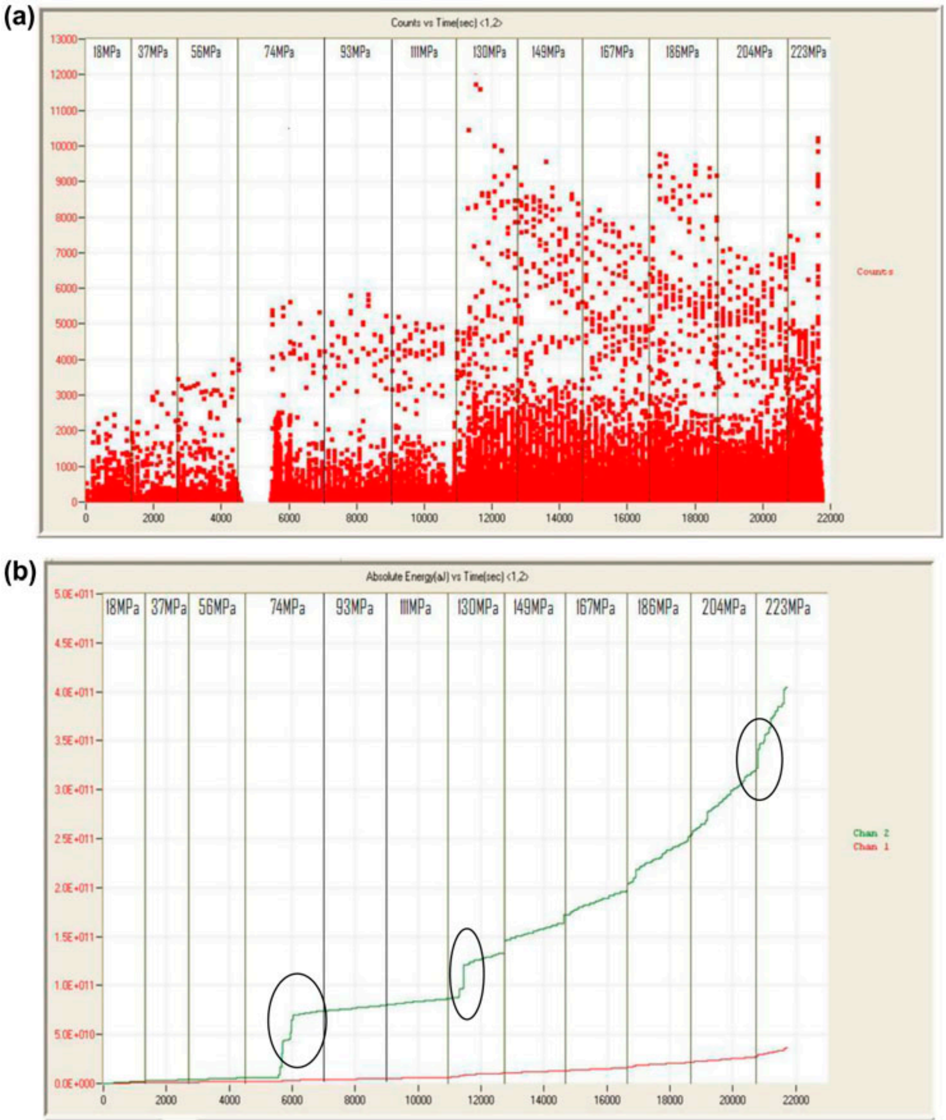

Figure 4. (a) change in AE counts and (b) cumulative energy counts throughout the UEWS test under hydrostatic loading (2:1).

Closer observation of the plot indicates that there are distinct three sharp rises in cumulative energy, firstly in the 4th cycle group at 74 MPa wall stress, secondly at 130 MPa wall stress and finally at the start of the 12th cycle group with a wall stress of 223 MPa. These correspond well with the previous AE count plot, confirming the onset and progression of damage. However, in order to characterise the damage mechanisms involved, the AE signal durations from transducer 2 were plotted against the signal amplitude, which afterwards generated into a 3D correlation plot against time as given in Figure 6. From Figure 6(a), most of the AE events were of low duration and low/

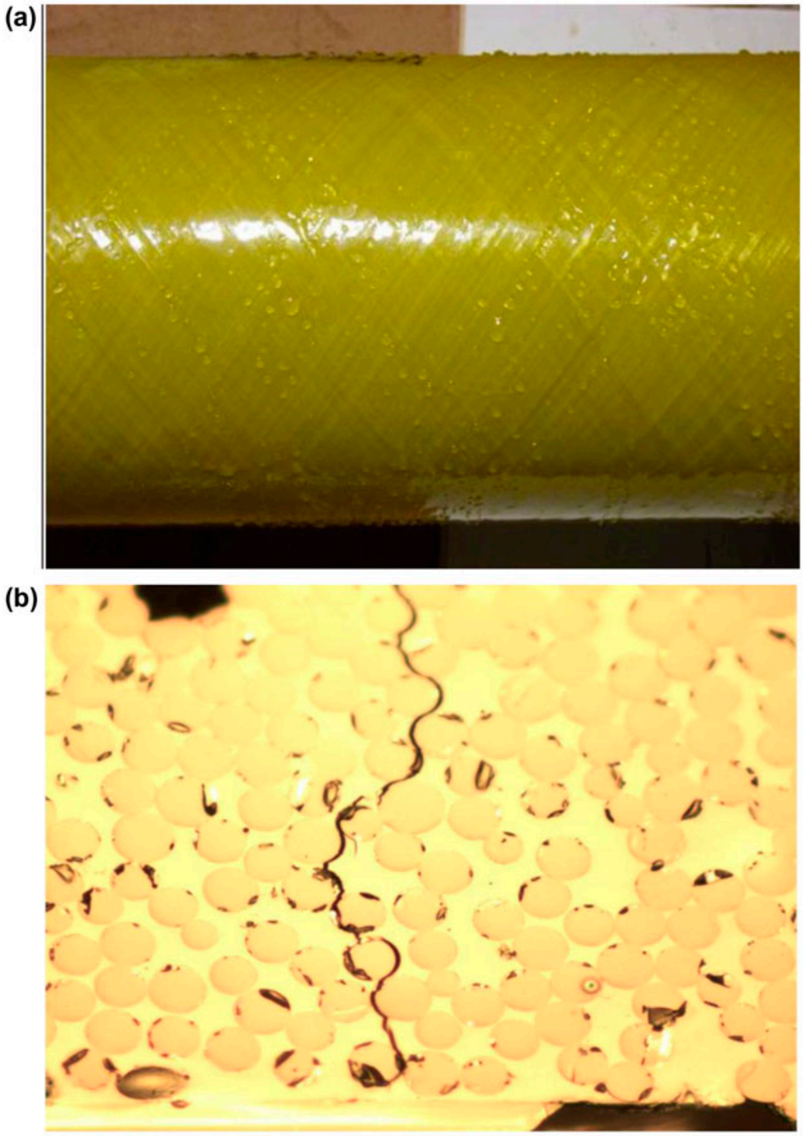

Figure 5. (a) Weepage failure of GRE pipes and (b) optical micrograph of transverse matrix cracks from polished weepage failure sample.

intermediate amplitude ranging from 45 to 85 dB as indicated in zone 1. This was attributed to the combination of matrix cracking and matrix–fibre debonding, and a 3D correlation in Figure 6(b) plot of these AE parameters against time suggests that these damage mechanisms took place throughout the test.

Small numbers of higher duration AE events were noted with amplitudes from 55 to 80 dB, as shown in zone 2. These events were suspected to be associated with friction between crack surface or resulting from fibre pull-out.[9] The 3D correlation indicates that, towards the latter stages of the test, events of low/intermediate duration were observed at high amplitudes between 90 and 120 dB (zone 3), which is likely to

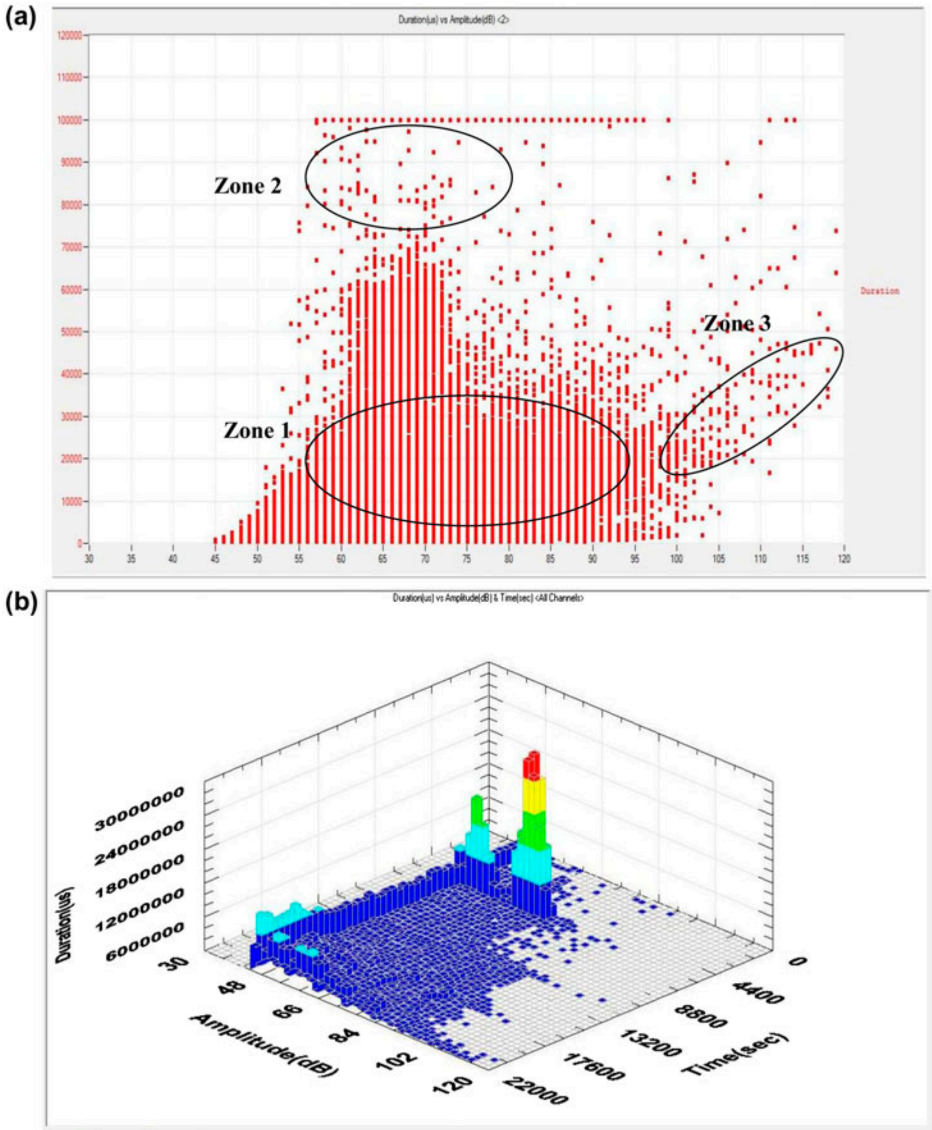

Figure 6. Plot of (a) AE duration against AE amplitude and (b) 3D correlation plot of AE duration vs. amplitude vs. time for UEWS test under hydrostatic loading (2:1).

be associated with delamination failure. All of these events were noted prior to weepage failure. The plot also suggests the possibility that fibre breakage might have taken place in zone 3, indicated by the low duration of high amplitude AE events (115–120 dB),[8] although this would have to be to a limited extent otherwise bursting would have happened instead of weepage. These failure mechanisms deduced from the AE data correspond well with the failure sequence prior to weepage as observed by previous researchers.[18–23]

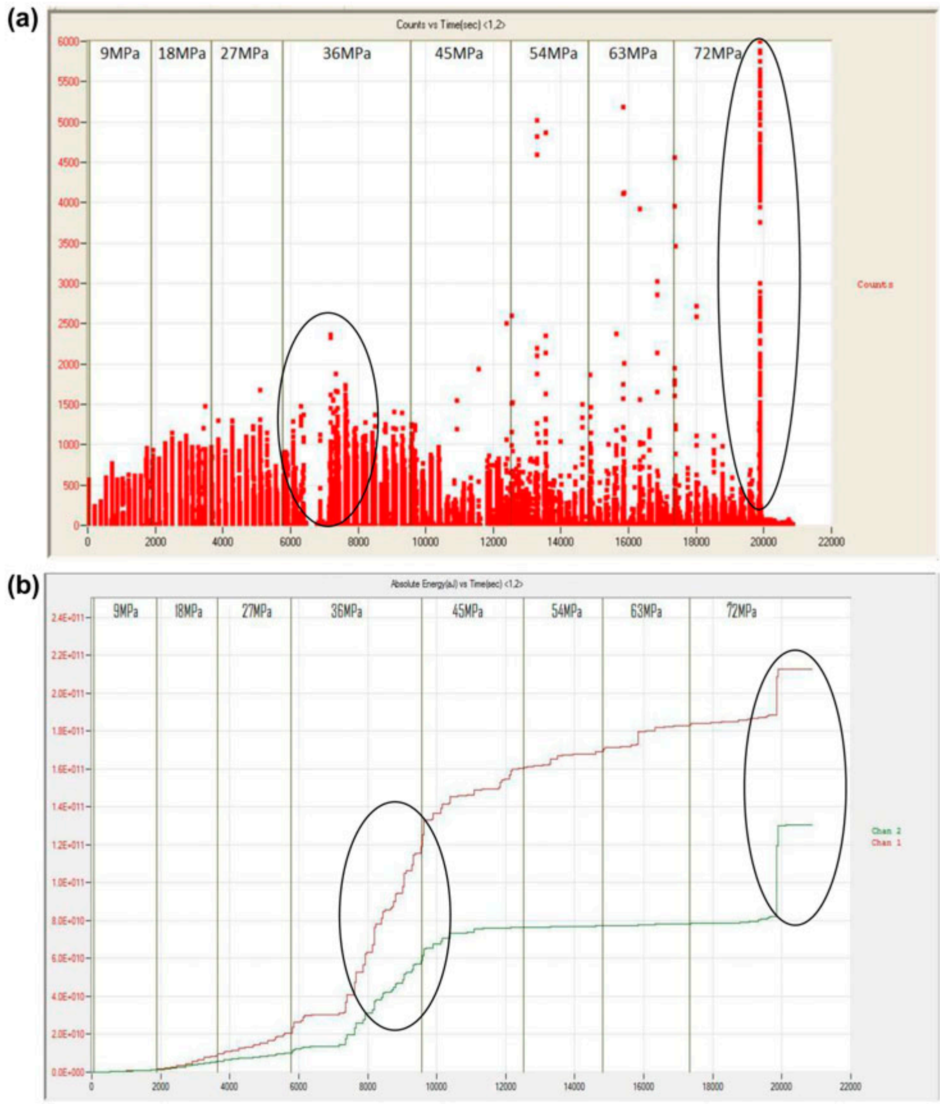

Figure 7. Plots of (a) change in AE counts and (b) cumulative energy throughout the UEWS test under pure axial loading (0:1).

3.2. Pure axial loading (0:1)

Figure 7 shows the AE counts and cumulative energy released during the UEWS test under pure axial loading (0:1). Similar to the results for hydrostatic loading, AE counts were observed from the first cycle group at a wall stress of 9 MPa, and these gradually increased with increasing pressure up to the 3rd cycle group of 27 MPa wall stress. A significant increase in AE counts was noted from the 4th cycle group at 36 MPa and this stabilised until the next cycle group at 45 MPa. This change in AE activity is believed to correspond to the onset of matrix-fibre debonds and matrix cracking. The

AE counts then increased considerably between the 6th and 7th cycle groups indicating the evolution of damage with counts reaches near 5500 although less than recorded in 2:1 loading test. Finally, the highest peak of AE counts was observed in the 8th cycle group as a result of fibre fracture due to tensile axial failure. A helical crack is evident along the fibre direction, extending along the middle section of the pipe and further pressurising caused the cracks to propagate parallel to the winding angle, and the pipe then subsequently fractured.

The cumulative energy plot also shows that most of the AE signals were captured by probe 1, suggesting that damage initiation and evolutions were taking place closer to this probe. Two distinct rises in cumulative energy were noted, first at 36 MPa wall stress and second in the final cycle group corresponding to tensile axial failure at 72 MPa. The change in cumulative AE energy showed a similar trend to the previous AE count plot, confirming the onset of damage and its progression in pure axial loading.

Plots of AE event durations against amplitude and the 3D correlation plot of these parameters against time are given in Figure 8. Since most AE events were detected near to transducer 1, these plots were generated from the signals gathered by this transducer. The plots show that most of the AE events were of low duration and low amplitude in the range of 45–80 dB similar to those observed with pure hydrostatic loading. These events can be seen in zone 1 and were normally associated with matrix cracking and matrix-fibre debonding. Intermediate/high duration events from 60–75 dB in zone 2 correspond to further debonding process and the rapid progression of matrix cracking which, according to the 3D correlation, were taking place between 6000 and 13,000 s. This means that the surge observed in the cumulative energy plot during this period can now be attributed to this debonding process. Some of the low-amplitude events of higher duration recorded here might also result from friction effects at the crack surfaces.[24] As indicated in [17], the final failure observed in this type of loading was tensile axial failure in the form of macro helical cracks, where obvious fibre breakage had taken place. Hence, high amplitude events between 85–110 dB of low/intermediate duration indicated in zones 3 and 4 can now be attributed to delamination failure and fibre breakage, respectively. The 3D correlation plot generated was also in conformity, indicating that these events occurred right at the end of the test just before final failure.

3.3. Pure hoop loading (1:0)

Figure 9 illustrates the changes in AE counts against time and cumulative energy for pure hoop loading (1:0) in the UEWS test. Similarly, the plot shows that AE activity started very early in the test. However, one apparent difference compared to the previous AE plots for hydrostatic and pure axial loading is that the number of counts did not gradually increase but instead remained fairly stable in distribution with no clear indication of damage initiation and progression. This implies that the sequence of damage mechanisms involved was somewhat different from those seen with 2:1 and 0:1 loading. The AE counts remained stable until the start of the 7th cycle group at 251 MPa wall stress when a sudden increase in counts was noted, reaches about 7000 at 9000 s, suggesting significant events had occurred. This is believed to correspond to the buckling of the pipe after serious bending had taken place, especially near the reinforcement ends where stress concentrations were at their highest.

The cumulative energy plot shows continuous rapid increments in energy released, with no clear ‘knees’ observed. Higher cumulative energy was also released compared to the hydrostatic and pure axial loading conditions, especially in the early cycle

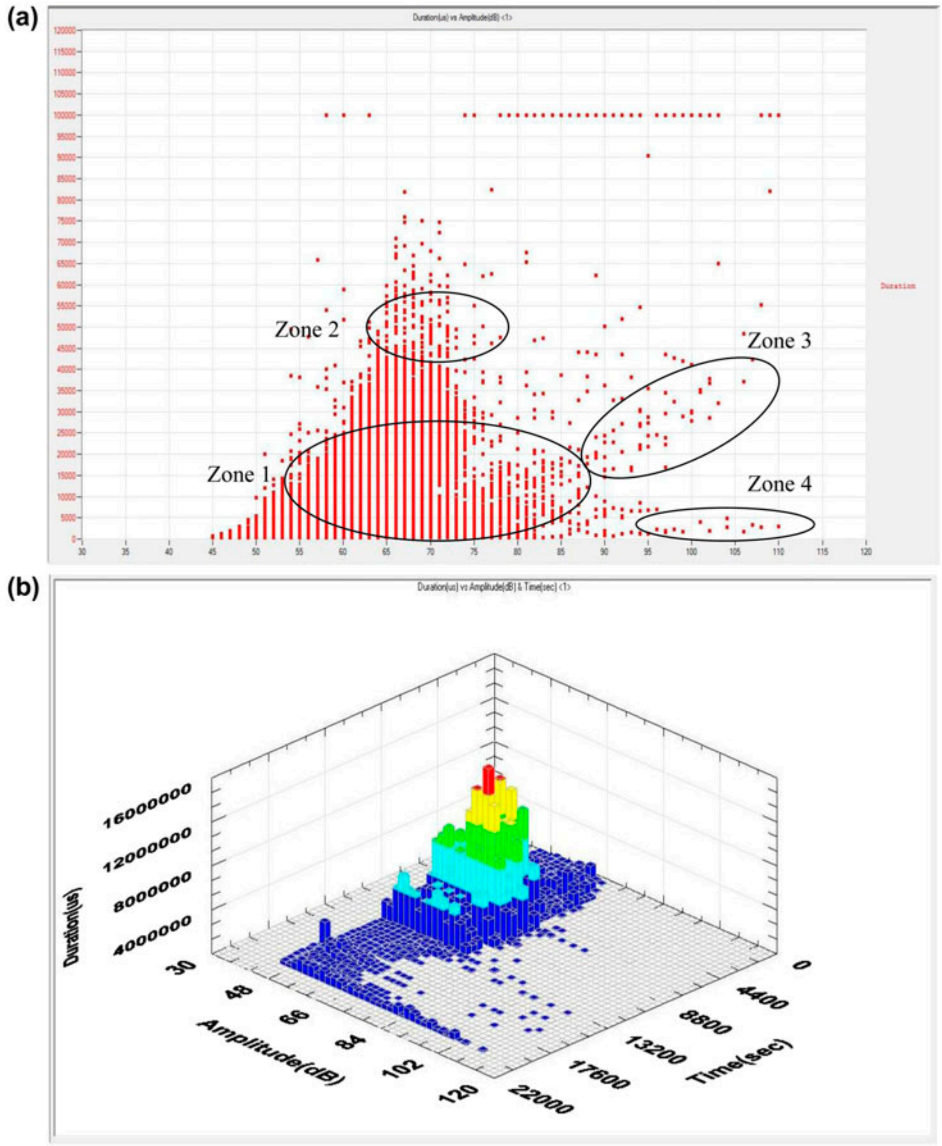

Figure 8. Plot of (a) AE duration against AE amplitude and (b) 3D correlation plot of AE duration vs. amplitude vs. time for UEWS test under pure axial loading (0:1).

groups. Once buckling failure took place in the 7th cycle group, fewer counts and lower energy releases were observed. This is because, after buckling failure, the continuing relatively high shear stress component caused shear deformation of the resin, which then resulted in secondary failure mechanisms such as matrix cracking.

Figure 10 shows the AE duration vs. amplitude and its corresponding 3D correlation plot of against time. The plots show that most of the AE events were of intermediate/high duration with intermediate/high amplitude ranging from 60–100 dB. These are

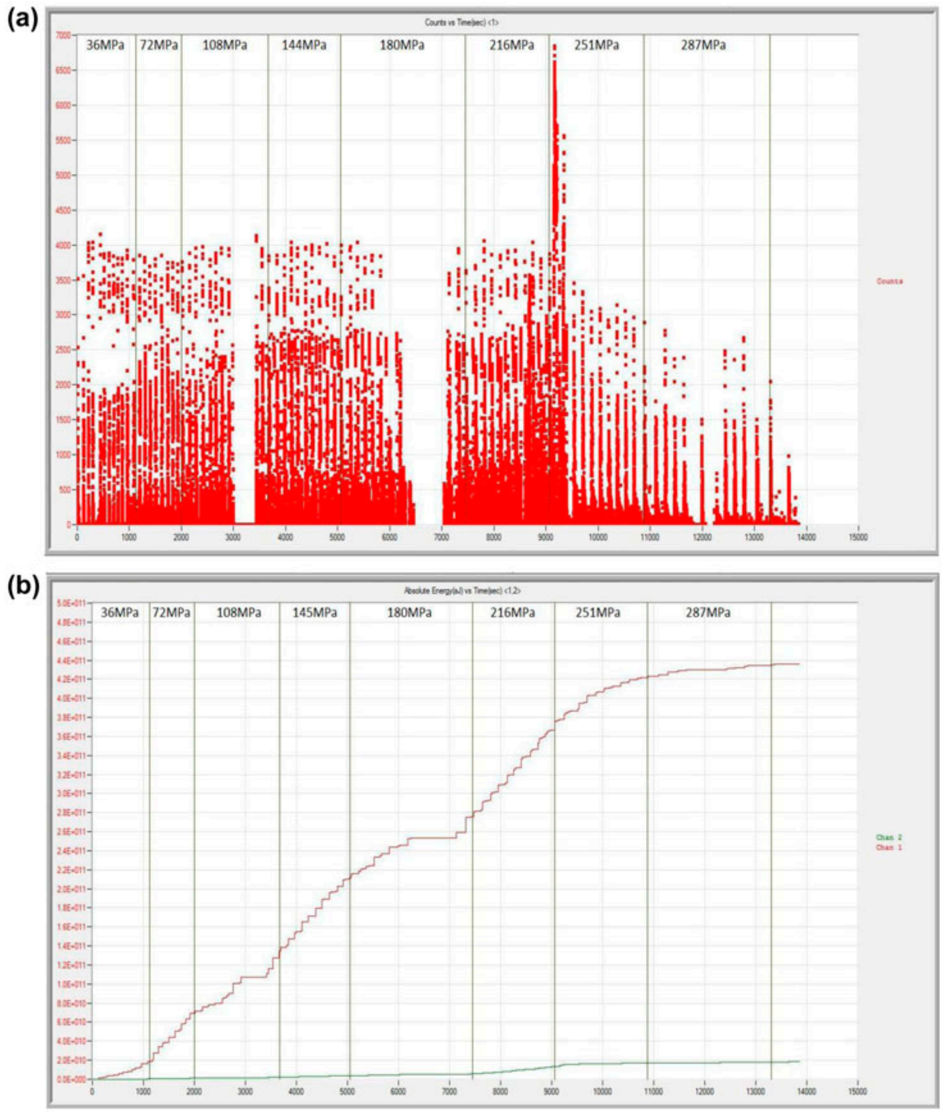

Figure 9. Plots of (a) change in AE counts and (b) cumulative energy counts throughout the UEWS test under pure hoop loading (1:0).

likely to correspond to the relatively high shear deformation of the resin matrix (zone 2). At about 9000 s into the test, massive delamination and debonding were generated near the end reinforcement, due to the pipe bending. This was quickly followed by buckling failure accompanied by the audible sound of fibre fracture on the outer surface of the pipe. This can be seen from the correlation plot, indicated by the peak of highest duration (due to friction) with a broad range of amplitudes up to 100 dB. The bending of the pipe just before buckling failure induced fibre breakage, and this is represented by the low duration, high amplitude AE events.[8] The plot also shows that, once buck-

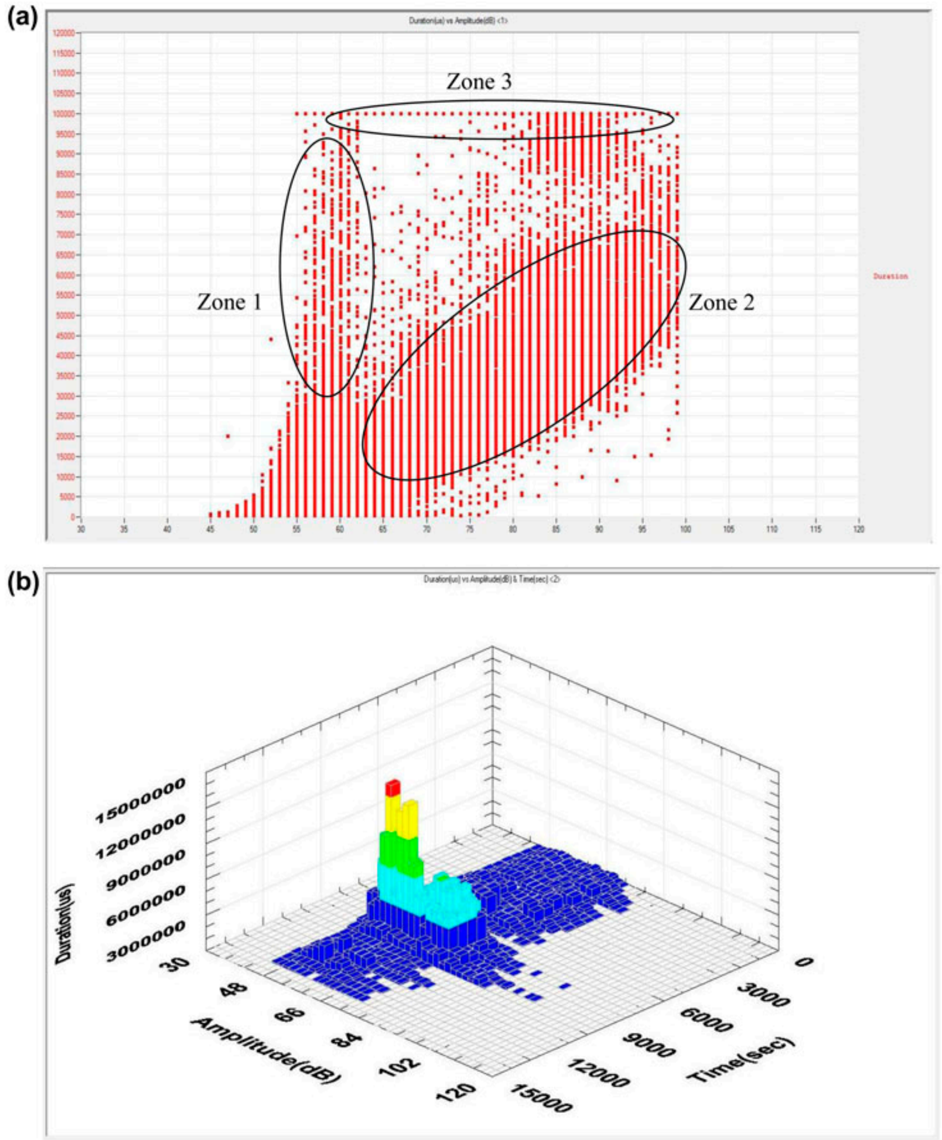

Figure 10. Plots of (a) AE duration against AE amplitude and (b) 3D correlation plot of AE duration vs. amplitude vs. time for UEWS test under pure hoop loading (1:0).

ling failure occurred, secondary failure mechanisms followed represented by events of low-amplitude and low/intermediate duration, which can be attributed to matrix cracking (zone 1), and events of high duration, low/intermediate amplitude (zone 3) which are normally associated with friction between crack surfaces.

4. Conclusions

AE measurements were conducted during the UEWS tests under hydrostatic, pure axial and pure hoop loadings at RT. The results for both hydrostatic and pure axial loadings indicate that matrix cracks were initiated and possibly had progressed to delamination immediately before the UEWS point was reached at 200 MPa of hoop stress and 63 MPa of axial stress, respectively. However, no clear damage initiation and progression was observed for pure hoop loading. Almost stable AE measurements were recorded, which is thought to be due to relatively high shear stress. Significant AE events were only noted when the bending of the pipe just before buckling induced massive delamination and debonding failure followed by fibre fracture on the outer surface of the pipe. As specified earlier, the objectives of the AE measurements were to characterise damage mechanisms involved at different stages of UEWS tests and to search for correlations between AE activity and the UEWS results. Through the analysis, the AE results do give good accounts on the states of damage mechanisms and progressions involved based on the distinct AE signatures throughout the test. The results hence suggest that, with further work, AE can be used as the monitoring tool to provide an early warning system for glass-reinforced plastics pipe failure.

This research is by no means comprehensive but an attempt to understand the AEs responses of GRE pipes when subjected to various loading ratios, hence inducing different failure controlling stress components within the laminates. Further work is required for characterising these damage mechanisms with more test experience is needed in order to decompose completely the interactions of these damage mechanisms with respect to its AE responses.

Acknowledgements

The work presented herein was supported by Future Pipes Industries, Netherlands, as part of a study of the performance of filament wound GRE pipes under Grant RES/0590/7256. The authors also would like to acknowledge the financial support from the overseas postgraduate programme of the Universiti Malaysia Perlis (UniMAP), Malaysia.

References

[1] Hull D, Legg MJ, Spencer B. Failure of glass/polyester filament wound pipe. Composites. 1978;9:17–24.
[2] Guild FJ, Walton D, Adams RD, Short D. The application of acoustic emission to fibre-reinforced composite materials. Composites. 1976;7:173–179.
[3] Williams JH, Jr SL. Acoustic emission monitoring of fiber composite materials and structures. J. Compos. Mater. 1978;12:348–370.
[4] Giordano M, Calabro A, Esposito C, D'Amore A, Nicolais L. An acoustic-emission characterization of the failure modes in polymer-composite materials. Compos. Sci. Technol. 1998;58:1923–1928.
[5] Yu Y, Choi J, Kweon J, Kim D. A study on the failure detection of composite materials using an acoustic emission. Compos. Struct. 2006;75:163–169.
[6] Huguet S, Godin N, Gaertner R, Salmon L, Villard D. Use of acoustic emission to identify damage modes in glass fibre reinforced polyester. Compos. Sci. Technol. 2002;62:1433–1444.
[7] Godin N, Haguet S, Gaertner R, Salmon L. Clustering of acoustic emission signals collected using tensile tests on unidirectional glass/polyester composites using supervised and unsupervised classifiers. NDT and E Int. 2004;37:253–264.
[8] Barré S, Benzeggagh ML. On the use of acoustic emission to investigate damage mechanisms in glass-fibre-reinforced polypropylene. Compos. Sci. Technol. 1994;52:369–376.

[9] Barnes CA, Ramirez G. Acoustic emission testing of carbon fibre composite offshore drilling risers. 6th International Symposium on Acoustic Emission from Composite Materials (AECM-6);1998:13–22.

[10] Czigány T. Special manufacturing and characteristics of basalt fiber reinforced hybrid polypropylene composites: mechanical properties and acoustic emission study. Compos. Sci. Technol. 2006;66:3210–3220.

[11] De Rosa Igor M, Santulli C, Sarasini F. Acoustic emission for monitoring the mechanical behaviour of natural fibre composites: a literature review. Composites Part A. 2009;40:1456–1469.

[12] Khalifa AB, Zidi M, Abdelwahed L. Mechanical characterization of glass/vinylester ±55° filament wound pipes by acoustic emission under axial monotonic loading. C.R. Mec. 2012;340:453–460.

[13] Liu PF, Chu JK, Liu YL, Zheng JY. A study on the failure mechanisms of carbon fiber/epoxy composite laminates using acoustic emission. Mater. Des. 2012;37:228–235.

[14] Prevorovsky Z, Landa M, Blahacek M, Varchon D, Rousseau J, Ferry L, Perreux D. Ultrasonic scanning and acoustic emission of composite tubes subjected to multiaxial loading. Ultrasonics. 1998;36:531–537.

[15] Ramirez G, Engelhardt MD, Fowler TJ. On the endurance limit of fiberglass pipes using acoustic emission. J. Pressure Vessel Technol. 2006;128:454–461.

[16] FuturePipes I. Engineering Guide for Wavistrong filament wound epoxy pipe systems. Wavistrong Engineering Guide. 2001.

[17] Abdul Majid MS, Assaleh TA, Gibson AG, Hale JM, Fahrer A, Rookus CAP, Hekman M. Ultimate elastic wall stress (UEWS) test of glass fibre reinforced epoxy (GRE) pipe. Composites Part A. 2011;42(10):1500–8.

[18] Jones MLC, Hull D. Microscopy of failure mechanisms in filament-wound pipe. J. Mater. Sci. 1979;14:165–174.

[19] Bailey JE, Parvizi A. On fibre debonding effects and the mechanism of transverse-ply failure in cross-ply laminates of glass fibre/thermoset composites. J. Mater. Sci. 1981;16:649–659.

[20] Meijer G, Ellyin F. A failure envelope for ±60° filament wound glass fibre reinforced epoxy tubulars. Composites Part A. 2008;39:555–564.

[21] Tarakcioglu N, Gemi L, Yapici A. Fatigue failure behavior of glass/epoxy ±55 filament wound pipes under internal pressure. Compos. Sci. Technol. 2005;65:703–708.

[22] Abdalla FH, Sapuan SM, Hamdan MM, Sahari B. Internal pressure carrying capacity for different loading modes of filament-wound pipes from glass fiber-reinforced epoxy composites. Polym. Plast. Technol. Eng. 2008;47:802–808.

[23] Mertiny P, Ursinus K. Damage behavior of joined fiber-reinforced polymer pipe under monotonic and cyclic loading. American Society of Mechanical Engineers, Pressure Vessels and Piping Division (Publication) PVP. 2008;2008:499–504.

[24] Pollock A. Acoustic emission inspection. Metals handbook. 9th ed. Russell Township (OH): ASM International; 1989. p. 278–294.